Carpathian Journal of Earth and Environmental Sciences, February 2017, Vol. 12, No. 1, p. 109 - 120

IRON RICH EMBEDDINGS IN EAST HUNGARIAN EOLIAN SAND ACCUMULATION, TAMÁSPUSZTA AREA: GENETIC AND ENVIRONMENTAL CONSIDERATIONS

János KALMÁR[1], György FÜLEKY[2], László KUTI[1] & András SEBŐK[2]

[1]*Geological and Geophysical Institute of Hungary, Budapest, johannkalmar@gmail.com, kutilaszlodr@gmail.com*

[2]*Szent István University, Gödöllő, fuleky.gyorgy@mkk.szie.hu, andras.sebok85@gmail.com*

Abstract: The ”kovárvány” called reddish, hardened embeddings of the eolian sand were examined. A few 10 cm thick, lens like or irregular bodies appear in the top of dunar morphology. They consist finer quartz sand with increased amount of clayey-silty grain size fraction and 0.5–1.2% iron content. In spite of the similar mineralogical composition of the sand fraction, differences appear in the shape and the size of the grains. The upper faces of these embeddings are gently waved, the grains are well packed, with nests of limonite concretions. The lower separation surface is irregular, often with a gradual passage to the host sand. In the SEM photos of the sand grains, biogenetical corrosion and crushing were evidenced. The bonding material with touching and void filling character consists of a colloidal mixture of iron hydroxides and clay minerals, while in the host sand, „free mason“ (cementless, uncemented?) and meniscus type bonding appear. The goethite and illite neoformation in the bonding material indicate the beginning of the diagenetic processes in this sediment. Neither ascending iron ions nor iron oxi-hidroxide precipitation was evidenced in the moving zone of the groundwater table. These embeddings represent the rest of ancient forest soil, with biogenetic iron accumulation and grain crushing. Thus, during the wet periods of the Holocene, the dunes were capped with small tree groups and bushes - and later, when the vegetation was dried out, the soil cover was partly eroded and it was buried under the moving sand nappes.

Key words: Dunar sand, grain size distribution, iron oxi-hydroxides, illite neoformations, biogenetical corrosion, forest soils, early diagenesis

1. INTRODUCTION

The eastern border zone of the Great Hungarian Plain and a large zone of the north-western Câmpia de Vest, between Secuieni and Berveni (Romania) are covered by Late Pleistocene eolian sand deposits.

Accepting the usual hypothesis about the genetics of these sand deposits, they were formed by the mobilization of the alluvia by the Tisa river-system, during the dry periods of the Upper Pleistocene and Early Holocene. The wind-blown sand form a specific dunar relief: the NW–SE to N–S oriented dunes reach 10 m height, with steep eastern and mild western slopes (Kalmár & Vatai, 1994). Based on the shallow borehole data, the actual groundwater table is situated at 128–132 m asl (above sea level), i.e. at 5–10 m under the dunes' surface (Kerék et al., 2001).

In the Romanian side of the state border line, Bulgăreanu (1968) distinguished an ancient, Pleistocene morphology that is overlay by the sub-recent and actual phase sand movements. According to the coverage of the site with Otoman (Ottomány) type potteries and boon fragments, respectively bronze vessels and weapons in western Bihor and Sălaj county (Romania), the last, massive sand movement happened probably in the II–III millennium, B.C. (Dumitraşcu, 1974).

In both sides of the state border, well sorted and clay free sand is used as a building raw material, exploited by inhabitants in small quarries and pits (Angelescu et al., 1984). However, in some sites, the dunes were crosscut by main or vicinal road excavations. In such a man made outcrops, into the light yellow, unstratified sand, lens like or irregular bodies of reddish brown separations were found. These separations were close to the actual dunar surface, not deeper than 2 meters.

These separations with increased iron oxi-

hydroxide content were described in this area as "*kovárvány*", i.e. a purely descriptive, popular term (Kádár, 1957), issued from the irregular form and varicolored feature of them.

There are a few hypotheses about the genesis of these accumulations, e.g. (i) Liesegang-type colloidal diffusion; (ii) ice lens in sand during the last permafrost period; (iii) descending accumulation of iron colloids below the groundwater table; and (iv) ascendant transport of iron colloids during the oscillation of the groundwater table.

Regarding the "kovárvány"-problem from sedimentological, mineralogical and pedological viewpoints, the genesis and the (paleo) environmental aspects of these deposits were emphasized in this paper.

Sampling these sediments to find the answer for the following questions, that should be targeted:

— What is the difference between the composition of the reddish brown ("kovárvány") and the yellowish sand levels?

— Are there proofs of iron oxi-hydroxide movement in the sediment?

— Are there relation between the iron oxi-hydroxide accumulation and the movement of the groundwater table?

— Is the iron accumulation process a superficial (pedological) or a deep (geological) phenomenon?

For answering the questions above about the sedimentological, mineralogical and chemical composition, 13 (bulk and undisturbed) sand samples were taken and analyzed.

2. LOCATION AND OUTCROPS

The area of Tamáspuszta is situated in the Tiszántúl Region (Eastern Hungary), on the right side of the Debrecen – Nyírbátor main road, at 15 km from Debrecen city (Plate 1, Fig. 1). In this area a largely waved plain developed at 140–150 m asl. Now, it is utilized as a sheep pasture. The vegetation is represented by scarce grass cover, insulated bushes and tree groups. At that place, on the steeper slope of a 3 m high dune, a few excavations (former sand pits) were dug, where the whole section of the dune buildup was opened and sampled.

The analyzed samples belong to the main section of the dune, where under a 5–10 cm humicsand layer, tree reddish-brown "kovárvány" levels were found and they were separated by more or less iron-poor, yellowish sand levels (Plate 1, photo 3).

Examining the digital photos under blue-green filter, the detailed geometry of these levels is evidenced. Both the upper and lower separation lines are sharp for each level. The upper one appears as a waved separation line, with 10–15 centimeters deep, strength cavities, suggesting small wind carved trenches. The lower line is sinuous, irregular, shown amplitude and gradual passage of 5–10 cm (Plate 1, photo 2). In three reddish levels, 5–30 cm large, irregular, worm-like, darker brown, hardened separations appear with increased iron content. Out of these continuous "kovárvány" levels, in the yellowish sand background, a few 10 cm large separations appear as lens like, slightly rounded, reddish brown bodies. It seems that both from the "normal" and from the darker "kovárvány" body, small pieces were detached and reworked in the upper yellowish sand.

3. THE SAMPLING AND THE ANALYZES OF THE SAMPLES

The sand samples were taken as a continuous, prism-like, 10×5 cm excavations from the wall of the pit. Apart from those, two, 5×5×2.5 cm undisturbed samples were extracted from the cap of the two lower iron rich sand levels. The grain size distribution was determined by sieving in a set of 2^n scale sieves. A few samples, in that the fraction of Ø<0.063 mm is lower, than 10%, the silt and clay fractions were analyzed by sedimentation (Köhn method).

The observations on the morphology of the sand grains, and the coating of them were taken using an optical (binocular) microscope and a scanning electron microscope (JEOL JSM-35, 25 KV). The X-ray diffractometric analyses of the Ø<0.063 mm fraction were executed using Philips PW 1730 diffractometer on natural, untreated material. The dark mineral phases, comprising mainly the iron oxy-hydroxides were studied in polished section, in reflected light.

4. RESULTS OF THE SEDIMENTOLOGICAL SAMPLING

The sedimentological study of these sandy deposits provides data about the transport and the deposition of the sediment grains of the studied dunar buildup. To reach this goal, the grain morphology, the grain size distribution and variation, and the packing of the grains were examined.

4.1. The morphology of the sand grains

Following the methods proposed by Molnár et al., (1995) for such sand deposits, the morphology of the individual grains was studied in loose sand under binocular microscope and with SEM photos (Figs. 1 and 2), while in undisturbed samples, with digital photos of thin section fields.

Plate 1.

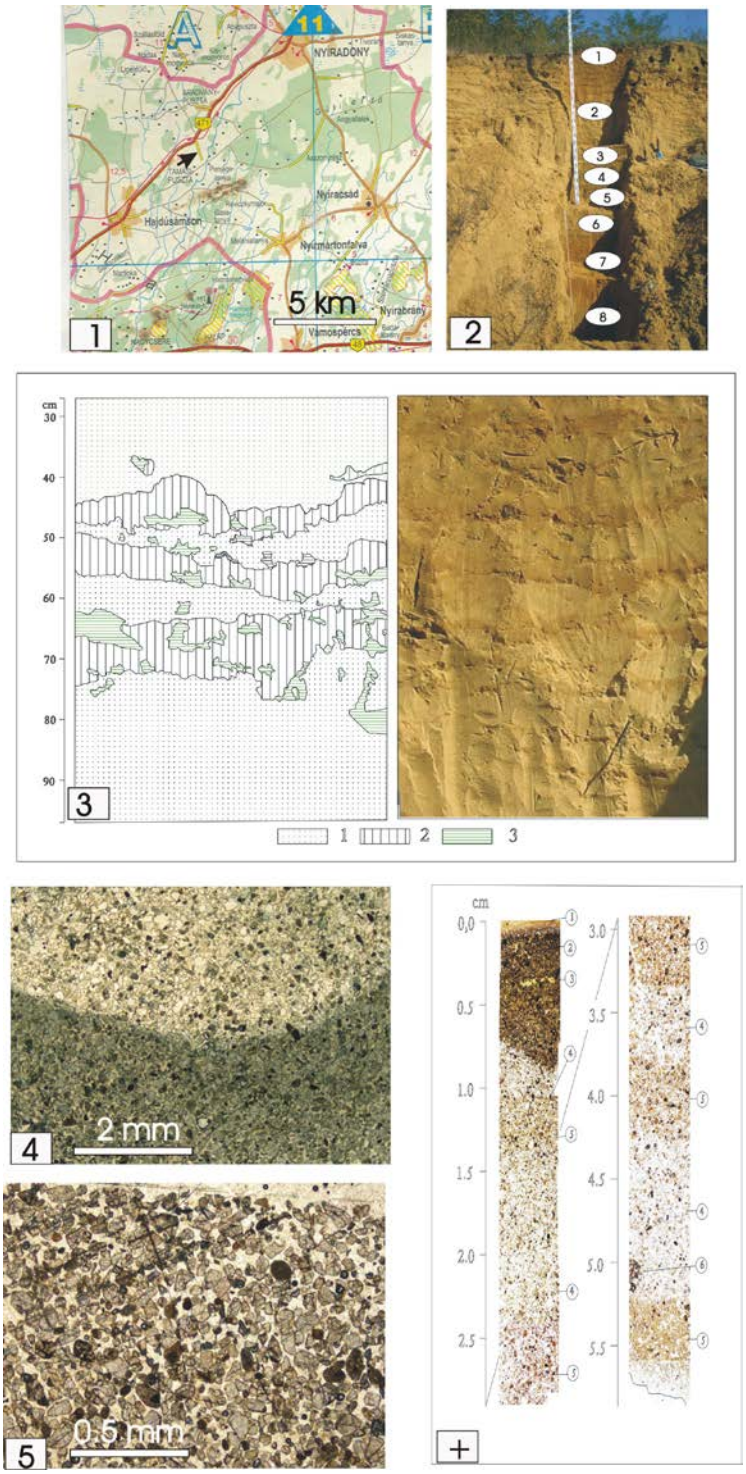

Figure 1. Location of Tamáspuszta area;

Photo 2. The sand samples of the outcrops (1-8);

Figure and Photo 3. The iron rich levels; in the right side, the photo of the outcrops; in the left side, the contour of these levels of the green filtered photo. 1. Iron poor, yellowish sand; 2. Iron rich, fine grained sand levels; 3. Dark brown, hardened sand with limonite and clay bonding separations.

Photo 4. Upper surface of the iron rich sand level No. 3, with strongly packed sand grains, thin section, II nicols;

Photo 5. Strong packed, coated, angular-subangular sand grains, limonite pellets, with slightly oriented texture; Cube 2 undisturbed sample, thin section, II nicols.

Photo 5. (+). Cross section in undisturbed sample Cube 2, with the detailed structure of the sand; seriated thin sections, II nicols: 1. Silty-clayey, limonitic lamina; 2. Strong packed, iron-rich sand with oriented texture; 4. fine-medium grained sand with scarce clayey limonite coating of the grains; 5. Loose, medium grained, nearly pure quartz sand; 6. Reworked fragment of fine grained sand with limonitic cement.

Table 1. Comparison of the grain shape between iron poor and iron rich sand samples

Grain shape	Iron poor sand		Iron rich sand	
	Grain number	%	Grain number	%
Isometric	185	60.06	175	47.43
Elongated	84	27.27	115	31.17
Prismatic	17	5.52	36	9.73
Platty	22	7.14	43	11.65
Total	308	100.00	360	100.00

Table 2. Comparison of the roundness between iron poor and iron rich sand samples

Roundness	Iron poor sand		Iron rich sand	
	Grain number	%	Grain number	%
Rounded	52	5.86	41	8.38
Subrounded	303	34.12	145	29.65
Subangular	345	38.85	142	29.04
Angular	188	21.27	161	32.92
Total	888	100.00	489	100.00

Knowing that the grain size distribution in the Ø0.1–0.3 mm fractions represents nearly the ⅔ part of the total grains, the shape and roundness of these fractions were studied here. Grains with the size <Ø0.1 mm are mainly angular, splint like, while grains up to Ø0.3 mm are composite ones, where the polished faces alternate with sharp irregular fracture surfaces.

Comparing the shape of the sand grains from the iron rich levels with those from the host sand, significant differences appear (Table 1). Among the grains of iron rich sand, the amount of the elongated, prismatic and platy grains increases at the expense of isometric ones. Similarly, the roundness of these grains differ (Table 2), with a relatively high amount of angular, and sharp edged grains in iron rich samples.

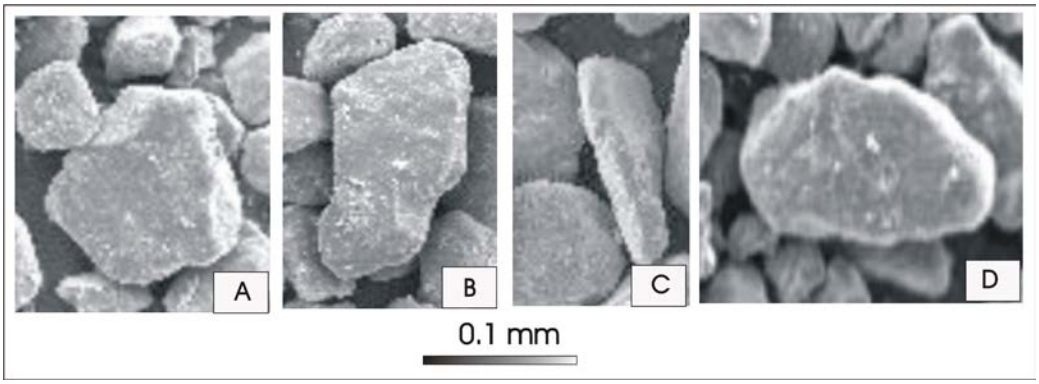

Figure 1. Examples of sand grain shapes. A. Isometric; B. Elongated; C. Prismatic; D. Plate grains. SEM photos: A and C from sample No. 3; B and D from sample No. 8.

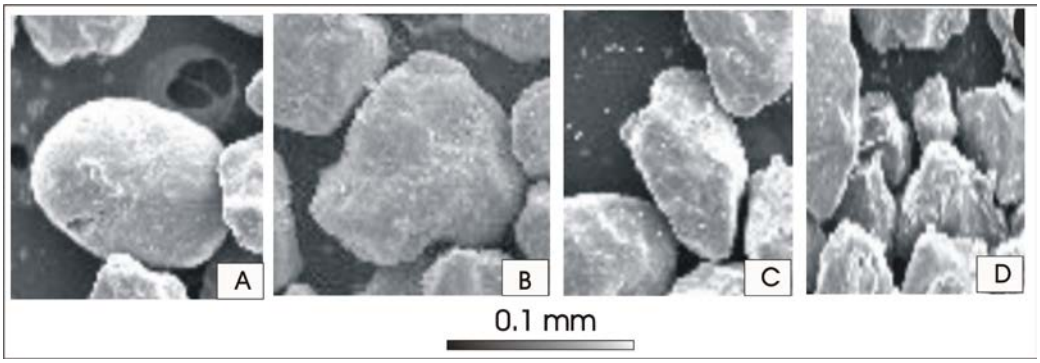

Figure 2. Example of roundness of the sand grains. A. Rounded; B. Subrounded; C. Subangular; D. Nest of angular, split-like grains. SEM photos: A and B from sample No. 2; C from sample No. 8 and D from sample No. 7.

Both morphological different must be judged in terms with the difference between the grain size distribution of these sediments: the sand of the "kovárvány" levels are rather finer, than the host sand (see below).

On the highly magnified SEM photos about the different sand grains, either the aspect of the grain surface or the coating can be observed.

Thus, the well rounded quartz grains of iron poor, host sand (Plate 2, photo 1) show smooth surfaces, with thin stria marking the internal structure of the metamorphic quartz — and rare star-like percussion fissures proving the eolian abrasion effect. On the surface rare plate-like, 10 micron sized chert nodules (as a heritage of the fluvial transport, see Walker & Douglas, 1984), clay and limonite adherences can be observed. In opposite to these smooth grains in the iron rich sand, highly corroded grains appear with complicate, irregular surfaces (Plate 2, photo 2).

The metamorphic quartz grains are grooved by 1–3 μm deep channels (plate 1, photo 3), often filled with scale like clay minerals and thin goethite needs (Plate 2, photo 5). While the majority of the grains of yellow, iron poor sand are barren, these are coated in the iron rich sand. Thin, folded clayey-colloidal films appear too (Plate 2, photo 4), and the coating is fragmented by a network of contraction (drying) cracks (Plate 2, photo 6). Grains with limonite rims also appear in thin and polished sections (Plate 1, photo 5; plate 3, photo 6).

4.2. Grain size distribution

Based on the grain size distribution, these sediments show a sandy character, with a small amount of finer (clayey and silty) fractions (Table 3). The slightly increased quantity of <Ø0.002 mm clay fraction and 0.02–0.06 mm silt fraction characterizes the dark colored, iron bearing ("kovárvány") levels, where the fine sand fraction dominates. In ternary diagram the samples plot in different fields (Fig. 3) after Füchtbauer & Müller (1970).

From the cumulative distribution of the grain size (d) using the method proposed by Folk & Ward (1957), the characteristic parameters of the distribution were calculated: i.e. the mean grain size (M_z), the dispersion of grain size values (σ), the skewness (S_k) and the pointednes of them (K_G). In table 4, these parameters are presented in φ values ($\varphi=-\log_2 d$). The differences between the iron bearing and the iron poor sediments are evident.

As suggested by Friedman (1961), the correlative groups of these parameters provide some structural and genetical information about the sampled sediment. Ordered pairs were created from the parameters like M_z/σ, M_z/S_k S_k/σ and S_k/K_G. On the diagrams of three of them the iron rich and iron poor sand can be separated (Fig. 4).

4.3. Stratification and structure

Regarding the scale of the outcrops, the iron rich levels appear as conformly imbedded, finer, well packed, more or less irregular lenses in the iron poor, loose, coarser host sand mass. As it was mentioned previously in the previous section, there are significant differences between the grain size parameters. The differences persist on the scale of a few cm thin levels ("lamina"). While the iron rich sand levels in the undisturbed samples Cube 1 and Cube 2 are built up by the succession of a few mm thick silty and sandy laminas with darker lenses of small limonite pellets (Plate 1, the top of the Fig. 6), the iron poor, coarser, loose host sand is characterized by 1–2 cm thick levels of white sand with "free mason" structure and light yellowish levels with slightly clayey-limonitic meniscus bonding alternate. This structural aspect characterizes the loose, wind-blown sand accumulations (Pettijohn et al., 1973).

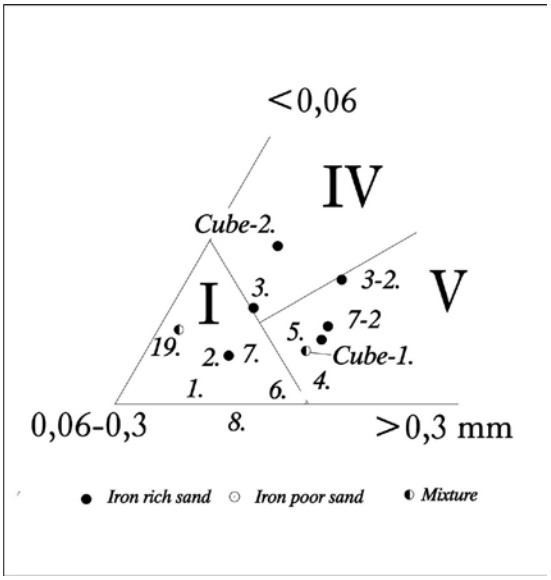

Figure 3. The left corner of the ternary diagram after Füchtbauer & Müller (1970), I. Fine grained sand; IV. Silty, fine grained sand; V. Fine grained – medium to coarse grained sand.

In the undisturbed samples, a weak grain orientation could be observed in the sand, while in the iron rich lenses moved and balanced grains appear (Plate 3, photos 2 and 4) as the effect of the compaction and packing. The dark limonite pellets are lineated (Plate 1, photo 5).

The upper boundary of the iron rich sand levels is marked by a strongly packed, fine grained,

hardened lamina. At the lower boundary, a few cm transition zone is formed, where the packing and the content of the fine grained fractions decreases gradually (Plate 1, photo 4).

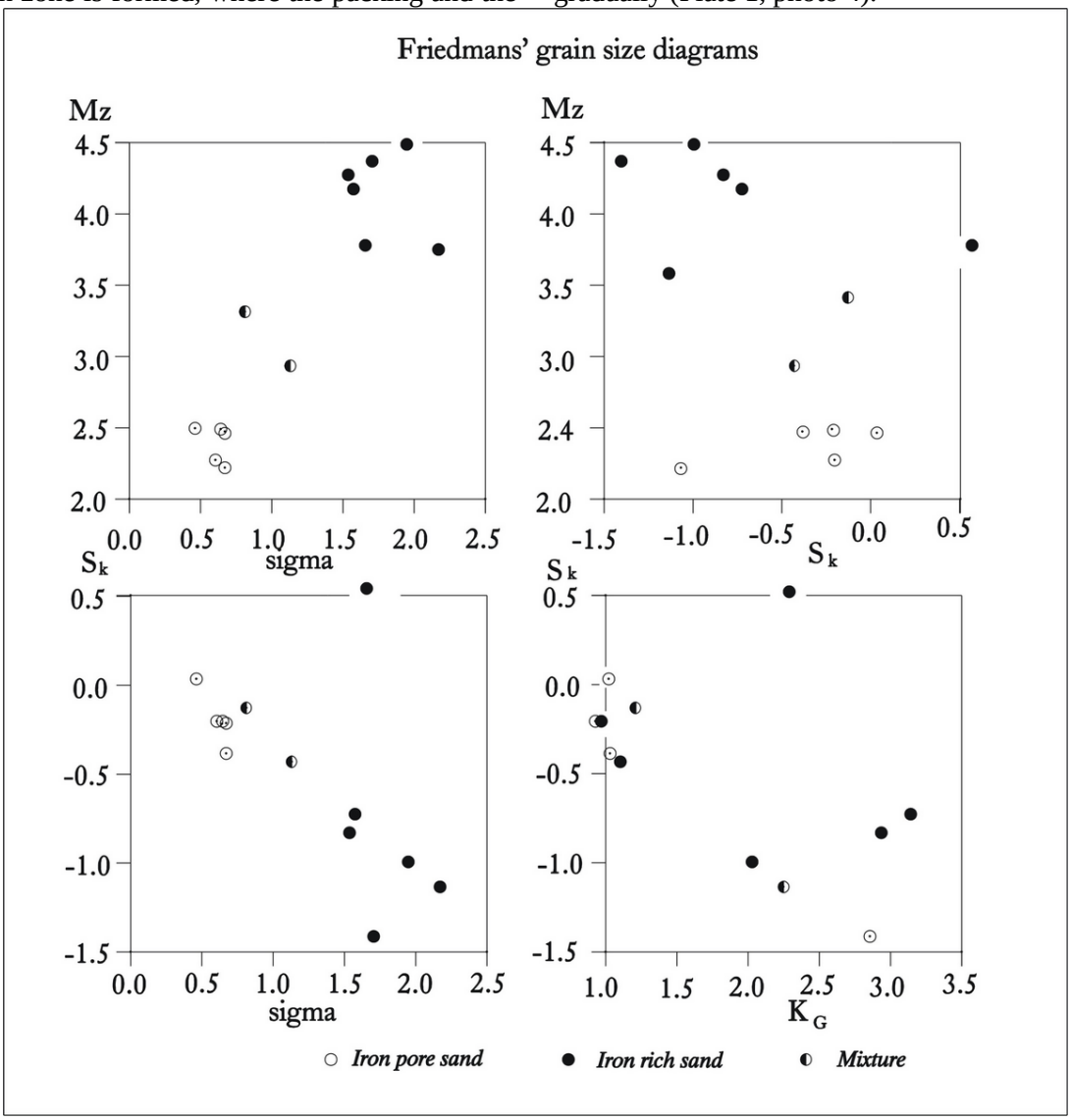

Figure 4. Friedmans' grain size diagrams grouping the iron rich and the iron poor sand samples.

Table 3. Grain size distribution of sand samples

Depth. cm	Iron oxydes	Grain size. mm											
		0.00–0.002	0.002–0.005	0.005–0.01	0.01–0.02	0.02–0.06	0.06–0.1	0.1–0.2	0.2–0.3	0.3–0.5	0.5–1.0	1.0–2.0	2.0–3.0
5–20		1.8	0.6	0.2	0.2	0.5	4.5	38.1	45.5	8.2	0.4		
20–35		1.5	0.3	0.2	0.3	0.9	5.4	41.6	40.3	8.1	1.2	0.2	
35–50	present	5.9	0.8	0.4	1.0	3.7	4.1	30.8	44.8	8.3	0.2		
50–65		0.6	0.2	0.2	0.1	0.3	3.4	34.7	41.6	18.0	0.9		
65–75	present	6.0	1.0	0.4	0.2	0.4	3.1	31.7	39.8	17.1	0.3		
75–90		1.0	0.3	0.2	0.2	.3	3.2	40.4	40.9	12.8	0.7		
90–100	present	8..8	1.2	0.5	0.3	4.3	3.4	30.3	42.4	8.5	0.3		
100–110		0.3	0.2	0.2	0.1	0.3	2.1	41.4	44.0	10.6	0.8		
35–50	present	8.8	2.1	1.8	0.5	2.0.	23.4	32.4	12.7	4.1	6.4	5.6	0.2
90–100	present	5.5	2.0	0.3	0.5	1.2	24.7	29.5	18.6	7.8	3.8	5.7	0.4
Cube 1	mixture	2.2	0.5	0.8	0.5	2.5	22.2	27.9	26.5	13.2	3.5	0.2	
Cube 2	present	5.3	2.2	3.5	3.3	5.0	23.4	30.2	19.6	3.5	3.3	0.3	0.4
19-23	mixture	0.8	0.2	0.2	0.3	7.6	26.8	55.5	6.4	2.0	0.2		

Plate 2. SEM photos

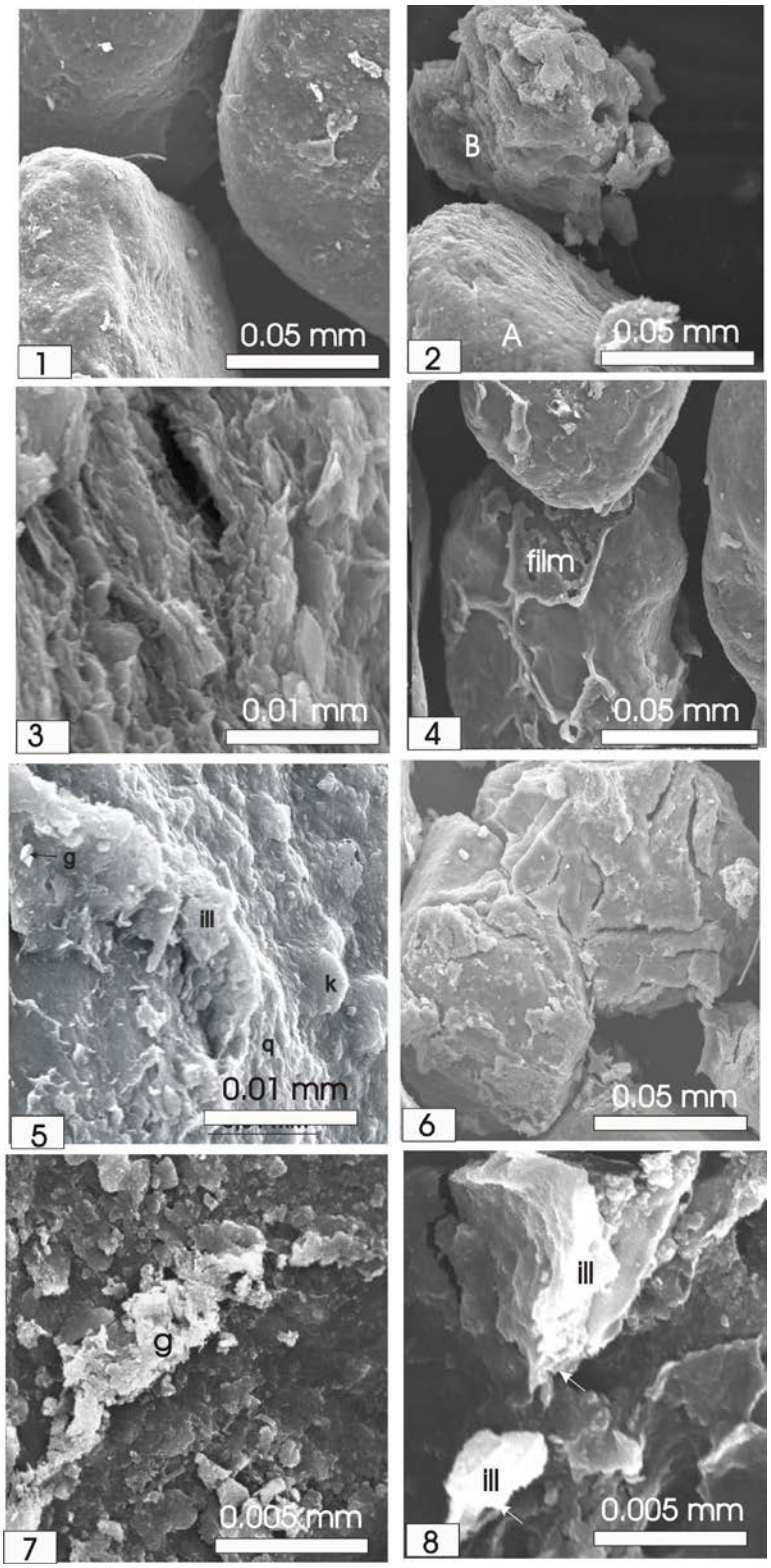

Photo l. Rounded, smooth quartz grains, sample 8. On the right grain a star-like percussion fissures can be seen;
Photo 2. Well rounded (A) and irregular, highly corroded quartz grains (B) from sample 3;
Photo 3. Deep corrosion channels on quartz grains from sample 3?;
Photo 4. Thin, folded and disrupted clay-limonite film on an elongated feldspar grain, from sample 7;
Photo 5. Illite (ill), kaolinite (k) and very fine goethite needs on the corroded quartz grain, sample 8;
Photo 6. Drying cracks on the colloidal coating of a sand grain; sample 7;
Photo 7. Euhedral goethite crystal aggregate on a quartz grain surface, sample 3.

Table 4. Distribution parameters of the samples; the **Bold** characters mark the iron rich ones

Sample No.	Depth. cm	Iron oxydes	Characteristics			
			M_z	σ	S_k	K_G
1	5–20		2.473	0.671	–0.387	1.032
2	20–35		2.464	0.462	0.032	1.022
3	35–50	present	4.274	1.536	–0.831	2.935
4	50–65		2.219	0.671	–0.217	0.960
5	65–75	present	4.174	1.574	–0.727	3.141
6	75–90		2.290	0.641	–0.220	0.932
7	90–100	present	4.370	1.705	–1.413	2.855
8	100–110		2.274	0.605	–0.206	0.928
3_2	35–50	present	3.917	2.171	–1.136	2.250
7_2	90–100	present	3.780	1.656	0.565	2.284
Cube 1		mixture	2.934	1.130	–0.433	1.103
Cube 2		present	4.488	1.948	–0.995	2.028
19	19-23	mixture	3.314	0.811	–0.130	1.213

Table 5. Mineralogical composition of the sand samples, resulted from optical analyzes

Sample No	Minerals, %								Rock fragments	Limonite	Plant fragments	Cement or matrix
	Quartz	K-feldspar	Plagio-clase	Musco-vite	Biotite	Amphi-bole	Chlorute	Accesso-ries				
1	92	4				present			1		3	present
2	90	5	2	present	present		present	present	present			3
3	86	5		1	present	present		present	present	present	1	7
4	80	8	2			1	1	1	4		present	3
5	90	4		present		1		present	2	present	present	3
6	90	3	1	present	1		1		present			4
7	83	6		1	present	present	present	present	present	2	2	6
8	90	4	present			present		present	present	present		6
Cube_1	88	3	3	1				1	2	present		2
Cube:2	83	3	2	present		1	present	1	3	2	1	4

5. MINERALOGY

The mineralogy of the sand samples was studied by optical means in the loose sand, in the undisturbed samples and in the harder fragments of the iron rich levels. The composition of the fine fraction of the samples was analyzed by X-ray diffractometry.

In table 5, the results of the optical study (binocular and thin section) are presented. All of the samples show the absolute dominance of quartz, followed by feldspars (microcline, orthoclase, albite, intermediary plagioclase) and rare micas, chlorite, amphibole and accessory mineral grains. The accessories are represented by zircon, titanite, rutile, staurolite, garnet, tourmaline, epidote and dark minerals. The lithoclasts (rhyolite, weathered basic igneous rocks, mica bearing quartzites, fine grained sandstone, marl and chert fragments) represent less than 4%. In some samples limonite pellets and crusts, and plant fragments with cellular structure were identified. The meniscus type or void filling, fine grained or colloidal bonding material reaches max. 6% in the iron rich samples. In the undisturbed samples, within iron free lamina Ø0.5–3.5 mm finer, rounded, strongly packed sand bodies appear, with sharp boundaries and with dark brown (limonitic or humic?) cement. They seem to be the clasts of the former iron rich sand levels, incorporated or reworked in the younger, iron poor host sand.

The dark mineral phase of the samples identified in the polished sections (Table 6) is represented by magnetite, hematite and ilmenite, often as highly corroded clastic grains, by limonitized (igneous?) rock fragments and by crusts and crowns around the sand grains, in that the colloidal limonite gel is recrystallized, forming small goethite prisms (Plate 3, photo 6). Goethite crystals appear also on the quartz grains in SEM photos (Plate 2, photo 7). In the polished sections, fine, micron sized needle-like, anisotrope, highly reflecting minerals appear in the colloidal bonding

Plate 3.

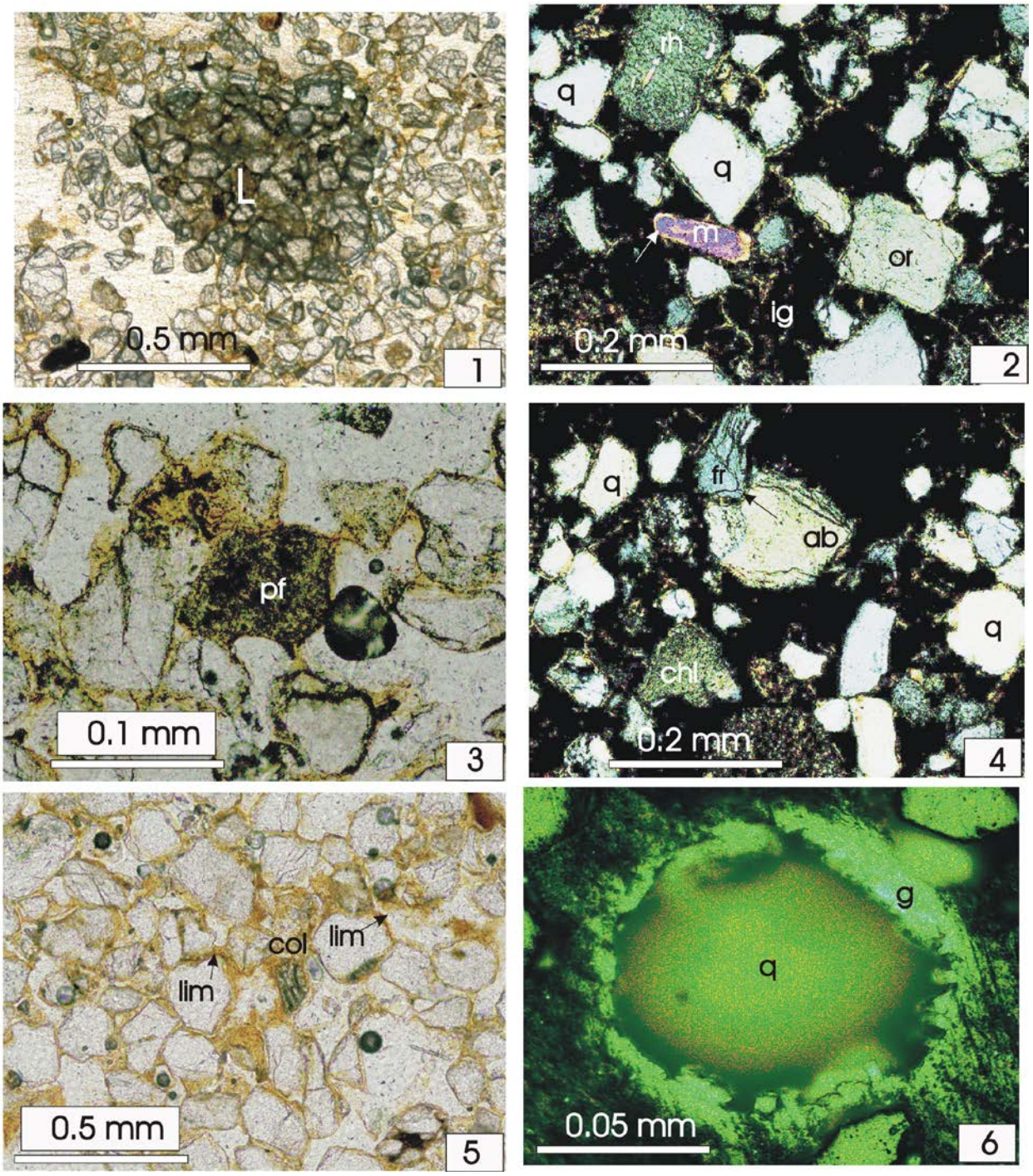

Photo 1. Lithic grain (L): reworked fine grained sand cemented with limonite. Cube 1 undisturbed sample, thin section, ll nichols;

Photo 2. Polymict, well packed sand in that the quartz grain (q) pinched and tilted over the muscovite plate (m). or, orthoclase; rh, rhyolite and ig, weathered igneous rock fragment. Cube 2 undisturbed sample, thin section, + nichols.

Photo 3. Plant fragment (pf) with cellular structure. Cube 1 undisturbed sample, thin section, ll nichols.

Photo 4. Compaction and grain movement: the quartzite fragment (fr) wipes down the clayey rim of albite (ab). Cube 2 undisturbed sample, + nichols.

Photo 5. Between two limonite coated quartz grains (lim) a plastic clayey-limonitic colloid was intruded (col). Sample 5, thin section, ll nichols.

Photo 6. Corroded quartz grain (q) with goethite rim (g). Sample 5, polished section.

among the sand grains. This is the first step to the formation of diagenetical goethite in the sediments (Cornell, 1986; Schwertmann & Cornell, 2000).

In the undisturbed samples, the host sand grains are bonded at their touching points by small meniscus with a clayey-limonitic composition. In the harder and finer iron rich levels, the bonding material forms rims around the grains or fills the voids between them, showing a zoned fluidal structure (Plate 3, photo 5).

The mineral composition of the <Ø0,063 mm grain size fraction appears in X-ray patterns (Table 7, Fig. 4) The fraction are represented mainly by fine quartz fragments and a relatively high amount of clay minerals and of amorphous mineral phase. The iron minerals show notable concentrations in samples 3, 7 and Cube 2.

As concerning the clay minerals, the presence of montmorillonite and illite pairs is notable, and the illite-montmorillonite mixed layer mineral as well (Table 7, Fig. 5). Both clay minerals show disordered lattice and implicit, a low degree of crystallinity, proper for soils (Mehring, 1975; Melkerud, 1986). In SEM photos, the newly formed illite appears as icicle like bodies on the edge of the illite flakes (Plate 2, photo 8).

6. CHEMICAL FEATURES

On the sand samples, humus analyzes, pH and differentiated extraction of the iron oxides was performed. The results are presented in table 8. The humus content is significant only in the uppermost soil level (samples No. 1–3), and falling under 0.1% values for the rest of the samples. Thus, the presence of the humic material is tied to the recent biological activity. The reaction of sand samples is slightly below to the neutral point, with pH values around 6.

The oxalate leaching (Fe_{ox}) extracts all of iron oxides, including the crystallized phase of them, while the extraction with dithizone (Fe_{dit}) mobilizes mainly the colloidal phase (Bohl et al., 1985). In this way, the ratio Fe_{ox}/Fe_{dit}, gives the degree of the crystallization of the iron minerals, i.e. the state of the geological evolution of them (Nemecz & Csikós-Hartyáni, 1995). Thus the ratio increasing from 0.80 (sample 2) to 1.17 (sample 8) proves, that there are an undisturbed, normal (geological) succession. Among them, the colloid bearing "kovárvány" levels 3 and 5 can be distinguished with the higher amount of the colloids.

Table 6. The dark minerals analyzed in polished sections Please write the table in the word.

Sample No.	Mineral phase					Limonitized rock fragments	Transparent mineral phase
	Magnetite	Hematite	Ilmenite	Goethite	Limonite		
2	present			present	2	1	97
3_1	2	3		2	3	present	90
3_2	present		present	3	3	2	92
7_1	1	1		present	2	present	96
7_2	2	present		2	5		91
8		presemt		1	1	present	98

Table 7. X-ray diffractometry analyses of the <Ø0,063 mm grain size fraction of the sand samples

Sample No.	2	3.	7.	8	Cube 2
Montmorillonite	present	4	5	2	6
Illite	2	6	10	3	10
Illite+montmorillonite mixed layer		present	2		2
Chlorite	present	4	3	present	4
Quartz	92	62	56	87	57
K-feldspar		1	2	3	3
Plagioclase		4	7	present	4
Goethite	2	5	4	present	2
Hematite	present	6	5	1	4
Gypsum		present		1	2
Amorphous	4	8	6	3	6
Total	100	100	100	100	100

Analyses executed by P Kovács-Pálffy and P. Kónya (MÁFI Lab., 2008-2015)

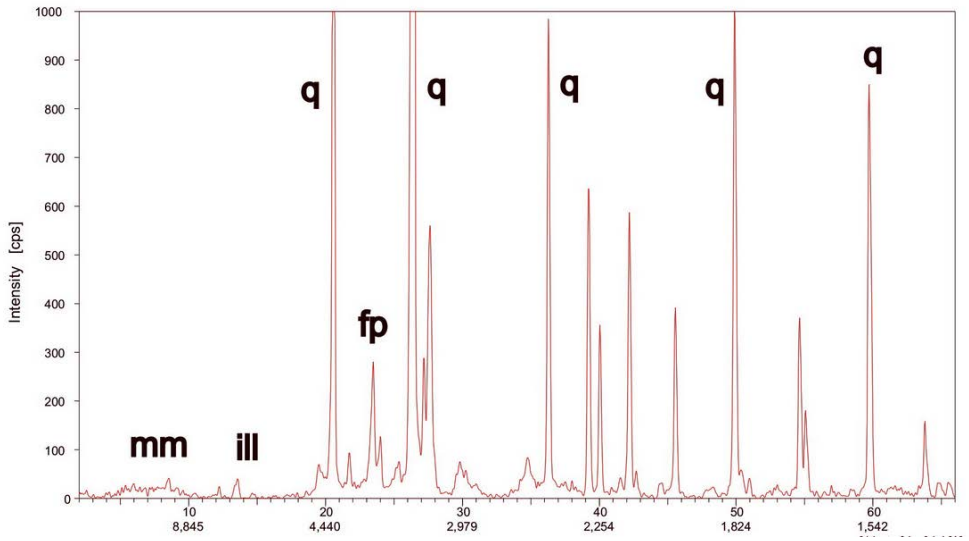

Figure 5. X-ray diffractometric pattern of sample No. 7, Ø<0,063 mm fraction, with peaks of main minerals: q, quartz; fp, feldspars; mm, montmorillonite; ill, illite. The lines of the XR is not intens

Table 8. Humus, pH and iron extraction analyzes for sand samples 1–8 (Laboratory of Szent István University, Gödöllő). The **Bold** characters mark the iron rich ones

Sample No	Humus content, %	pH H_2O	Fe_{ox} mg/kg	Fe_{dit} mg/kg	Fe_{ox}/Fe_{dit}
1.	0.33	5.40	472	434	1.09
2.	0.15	5.90	482	606	0.80
3.	0.11	6.00	1079	1254	0.86
4.	0.09	6.16	543	462	1.18
5.	0.01	6.39	831	998	0.83
6.	0.01	6.50	462	450	1.02
7.	0.01	6.40	792	719	1.10
8.	0.01	6.46	432	369	1.17

7. GENETIC AND ENVIRONMENTAL CONCLUSIONS

In the sampled outcrops, three main iron rich sand levels and a few smaller lenses were identified.

The upper surface of these is gently waved, with wind carved grooves, while the lower boundary is irregular, often passing gradually toward the yellowish host sand. The smaller reddish brown lens and the cm-sized fragments as well, seem to be the reworked pieces of the material of the main levels.

Often on the upper surface of the main levels hardened crusts appear, with strongly packed sand grains. They appear also as darker, harder and well cemented irregular bodies.

In spite of the close similarity in the mineralogical composition, there are significant differences between the grain morphology and the grain size distribution of the iron rich levels and the host sand. These differences are coming from the increased content of finer grain size fraction, i.e. the massive presence of the splint-like, sharp edged sand and silt grains, and of the highly corroded ones — as indubitable proofs of the biological fragmentation of the coarser quartz (and other mineral) grains in soils (Wilding et al., 1977).

Apart from iron ions coming from the weathering and corrosion of the iron bearing minerals (biotite, chlorite, amphibole, magnetite, hematite) and rock fragments, the presence of partly decomposed plant fragments and colloidal limonite indicate the biogenetic (pedological) origin of the increased iron content (Schwertmann et al., 1968) in these “kovárvány” levels, similarto the process leading to the formation of “bog type” iron accumulations (Borchert, 1960).

The so called “kovárvány” represents the ancient, buried sections of (probably forest) soils, in that the iron movement is limited to the filling of the voids among the sand grains. Therefore, neither notable iron transport from the deeper zone nor the oscillation of the groundwater table is proved in the case of the studied outcrops.

Based on the conclusion of these studies, the (geological and historical) past of the landscape of the whole dunar zone from Western Romania to

Eastern Hungary was characterized by small forest caps of dunes, that grew during the rainy periods and dryed out during droughts. The uppermost sampled soil level seems to be a "kovárvány" level in progress.

Finally, it must be noted, that diagenetic processes started by the recrystallization of iron bearing colloids, and by the neoformation of the clay mineral particles.

REFERENCES

Angelescu, I., Chelbea, D., Kalmár I. & Todor V. 1984: *Quartzose sand from Horea–Sanislău* (in Romanian). Materiale de Constructie, Bucureşti, 33., 2., 17–21.

Bohl, H., McClean B. & O'Connor G. 1985: *Soil chemistry. Chapter 3.5.3. Iron minerals* (in Hungarian). Mezőgazdasági Kiadó & Gondolat Kiadó, Budapest. 112–113.

Borchert, H. 1960: *Genesis of sedimentary iron ores.* Trans. Inst. Min. Metall. 69., London, 161–179; 530–539.

Bulgăreanu, C. 1968*: The eolian sands of Western Plain* (in Romanian). St. Cerc. Geol., Geogr. Geof., seria Geol., XXXVIII., 26–45. Bucureşti

Cornell, R.M. 1986: *The effect of silicate on the transformation of ferryhidrite into goethite and/or hematite*. 13th Congress International of Society of Soil Scientists, Hamburg, Abstr., p. 1441.

Dumitraşcu, S. 1974: *The repertory of monuments from Sălaj and Bihor County* (in Romanian) Muzeul Judeţean Bihor, 51., 1074–1078, Oradea

Folk, R.L. & Ward, W.C. 1957: *Brazos River Bar: A study in the significance of grain size parameters*. Jo.Sed. Petr., 27, 3–27.

Friedmann, G.M. *1961*: *Distinction between dune, beach and river sands from their textural characteristics.* J. Sed. Petr., 31., 4., 514–529.

Füchtbauer, J. & Müller, G. 1970: *Sedimente und Sedimentgesteine; Sediment–Petrologie*. II. Schweiz-bartische Verlag., p. 726, Stuttgart

Kádár L. 1957: *The problem of kovárvány-tipe sand* (in Hungarian)]. Földrajzi Értesítő, XXI., 17–25, Budapest

Kalmár J. & Vatai J. 1994: *The Fülöp-Nyírlugos agrogeological model area and the morhology of the sandy sediments* (in Hungarian). Debreceni Környezeti Napok, Abstr. 22–24.

Kerék B., Kuti L. & Vatai J. 2001: *Agrogeological and geoecological characterization of surface and near surface sediments and the groundwater movements in them in the North-Eastern part of the Great Hungarian Plain* (in Hungarian). Acta Geographica, Geologica et Meteorologica Debrecina, XXXV., 103–116., Debrecen

Mehring, J. 1975: *Smectites.* In: **Gieseking, J.E**. (ed.): Soil components. II. Inorganic components. Springer Verl., Berlin, New York, 7–119.

Melkerud, P.A. 1986: *Clay mineralogical comparisons of weathering profiles associated with spruce and birch stand*. Geol. Fören. Förhanding. 107. Stockholm, 301–307.

Molnár B., Fényes J., Novoszáth L. & Kuti L. 1995: *Application of the results of optical and scanning electron microscopic methods for grain-shape examination on Quaternary formations*. GeoJournal 36/2, 157–168.

Nemecz E. & Csikós-Hartyáni Zs. 1995: *Processes in soils and palaeosoils: a new method for the study of weathering*. GeoJournal, 36., 130–142.

Pettijohn, F.J., Potter, P.E. & Siever, R. 1973: *Sand and Sandstone.* Springer, New York, Heidelberg, Berlin, 133–135.

Schwertmann, U. & Cornell, R.M. 2000: *Iron Oxides in Field and in the Laboratory. Preparation and characterisation*. IId. ed., Wiley VHC., Weinheim, New York, Brisbaine, Singapore, Toronto, 67–91.

Walker, R.G. & Douglas J. 1984*: Sandy Fluvial Systems.* In: **Walker, R.G.** (ed.): Facies models. IId ed., Geosciences, Toronto, 71–92.

Received at: 09. 11. 2015
Revised at: 18. 09. 2016
Accepted for publication at: 30. 09. 2016
Published online at: 08. 10. 2016